

Article

Feasibility of DRNN for Identifying Built Environment Barriers to Walkability Using Wearable Sensor Data from Pedestrians' Gait

Hyunsoo Kim 

Department of Architectural Engineering, Dankook University, 152 Jukjeon-ro, Suji-gu, Yongin-si 16890, Gyeonggi-do, Korea; hkim13@dankook.ac.kr

Abstract: Identifying built environment barriers to walkability is the first step toward monitoring and improving our walking environment. Although conventional approaches (i.e., surveys by experts or pedestrians, walking interviews, etc.) to identify built environment barriers have contributed to improving the walking environment, these approaches may require time and effort. To address the limitations of conventional approaches, wearable sensing technologies and data analysis techniques have recently been adopted in the investigation of the built environment. Among various wearable sensors, an inertial measurement unit (IMU) can continuously capture gait-related data, which can be used to identify built environment barriers to walkability. To propose a more efficient method, the author adopts a cascaded bidirectional and unidirectional long short-term memory (LSTM)-based deep recurrent neural network (DRNN) model for classifying human gait activities (normal and abnormal walking) according to walking environmental conditions (i.e., normal and abnormal conditions). This study uses 101,607 gait data collected from the author's previous study for training and testing a DRNN model. In addition, 31,142 gait data (20 participants) have been newly collected to validate whether the DRNN model is feasible for newly added gait data. The gait activity classification results show that the proposed method can classify normal gaits and abnormal gaits with an accuracy of about 95%. The results also indicate that the proposed method can be used to monitor environmental barriers and improve the walking environment.

Keywords: deep recurrent neural network (DRNN); long short-term memory (LSTM); walkability; wearable sensing; inertial measurement unit (IMU)



Citation: Kim, H. Feasibility of DRNN for Identifying Built Environment Barriers to Walkability Using Wearable Sensor Data from Pedestrians' Gait. *Appl. Sci.* **2022**, *12*, 4384. <https://doi.org/10.3390/app12094384>

Academic Editors: Alberto Belli, Paola Pierleoni and Sara Raggiunto

Received: 9 April 2022

Accepted: 25 April 2022

Published: 26 April 2022

Publisher's Note: MDPI stays neutral with regard to jurisdictional claims in published maps and institutional affiliations.



Copyright: © 2022 by the author. Licensee MDPI, Basel, Switzerland. This article is an open access article distributed under the terms and conditions of the Creative Commons Attribution (CC BY) license (<https://creativecommons.org/licenses/by/4.0/>).

1. Introduction

Promoting physical activity is crucial for citizens' physical and mental well-being [1]. Considering citizens' daily physical activities, walking is the most common activity [2,3]. Thus, it can be regarded that walking more is linked to a healthier life. Various studies have indicated that walking has also been related to health benefits such as reducing obesity [4–6], managing diabetes [7,8], improving cardiovascular health [9,10], and improving people's quality of life [11,12].

Considering that citizens' daily physical activities generally occur in the built environment, it is essential to provide a proper built environment for physical activities and walking. To provide a proper built environment for improving walkability, there are two approaches: promoting facilitators and eliminating environment barriers [13]. Even if a walking environment can include sufficient facilitators, people may be hesitant to walk in a walking environment with barriers. Although walkability is a highly complex concept because the overall walkability of a specific environment (e.g., sidewalk or street) is the combination of multi-dimensional features, it is clear that environment barriers should be identified and eliminated to improve walkability [14,15].

To identify environmental barriers, government agencies have tried to apply various approaches such as inspection by experts, survey by pedestrians, walking audits, and self-reporting by pedestrians [15,16]. Although these approaches have contributed to

identifying numerous types of environment barriers, there may be several problems. First, these conventional approaches require time and a budget [14,15]. Especially, inspection by experts requires excessive financial expenditure when a governmental agency needs to monitor a walking environment in a continuous manner [15]. Second, in the case of self-reporting or interviews with pedestrians, there may be a subjective bias depending on the sampling of pedestrians participating in the survey [17]. Finally, these methods may omit specific environmental barriers since the conventional approaches are performed in an interval manner. For example, some barriers are constant objects (e.g., broken sidewalk) and others are spatial-temporal objects (e.g., a moving bike on a sidewalk).

To date, the advancements in sensing technologies can offer an opportunity for overcoming the limitations of the conventional approaches mentioned above. There are two main streams to identifying environment barriers. The first is a vision-based approach. Various methods have been developed to detect potential environment barriers. Generally, vision-based approaches have analyzed images of various environmental conditions [18–20]. In the analysis process, the approaches have been driven by rule-based criteria such as defective sidewalk regulations [15]. However, the environmental barrier is a relative concept, since each individual has their own characteristics, and there may be various situational contexts in the built environment [21,22]. Therefore, it is challenging to detect environmental barriers to walkability using one objective criterion [14]. In addition to analyzing images of the walking environment, vision-based approaches can automatically collect human behaviors that interact with external environmental conditions. Although these approaches have the potential to solve the problems of the conventional methods, the vision-based approaches may go through struggles from the process of collecting scenes that represent interactions between a pedestrian and a walking condition. There are two ways to collect pedestrians' gait images: shooting a walk scene (i.e., closed-circuit television (CCTV) or an experimenter takes photos) and mounting a camera on a pedestrian. The first method can require lots of CCTV or experimenters that may be costly and labor-intensive. In addition, the first method cannot capture an exact gait scene when an interaction between a pedestrian and a walking condition occurs.

The second approach is to utilize wearable sensors. Considering human behaviors during walking are affected by external conditions, abnormal external conditions that can be understood as an environmental barrier may cause abnormal behaviors in pedestrians [23]. The previous studies have already proven that there is a change in human behavior or response in the presence of external stimuli. For example, Kim et al. [15] investigated the relationship between abnormal behaviors and defective sidewalks by using pedestrians' walking data collected from an inertial measurement unit (IMU). Bisadi et al. [24] investigated the relationship between environmental barriers and physiological data such as the average of the Maximum Lyapunov Exponential (MaxLE) and heart rate values. Kim et al. [25] used various wearable sensors (i.e., EDA, gait patterns calculated as MaxLE, and blood volume pulse) to evaluate the neighborhood built environment. Zeile [26] measured walkability by combining biosensors and geospatial analysis.

Although the above-mentioned studies presented the potential uses of wearable sensors for detecting environment barriers by using physiological data, they mainly focused on the magnitude of signals. Human gaits are very diverse under the conditions of the walking environment. Human gait patterns are usually constant when there is no environment barrier. On the other side, the gait patterns on environment barriers may become abnormal [14–16].

Therefore, if we can differentiate between abnormal gaits and normal gaits, we can find the environmental barriers that cause abnormal gaits. Existing wearable-based methods mainly used the intensity of the response to differentiate between abnormal gaits and normal gaits [27]. Although the existing method has shown sufficient potential to detect the hazard, the intensity-based approach to the reaction does not sufficiently consider the various types of human gait. For example, some people may be very wary of environmental barriers (weakening the intensity of their responses), while others may be more sensitive to

environmental barriers [28]. A method that can distinguish abnormal gaits from normal gaits, including these personal characteristics, is needed.

The recent development of wearable sensor-based human activity recognition (HAR) can provide an opportunity to address the current limitations of environmental barrier identification. The HAR technology has generally been formulated [29]. As shown in Figure 1, the general data-processing flow for HAR consists of (1) collecting the activity-related data from wearable sensors during performing activities, (2) extracting relevant features that can describe the sensed information, (3) using a learning method using labeled data, and (4) applying the learning method to new unknown data for HAR [29,30].

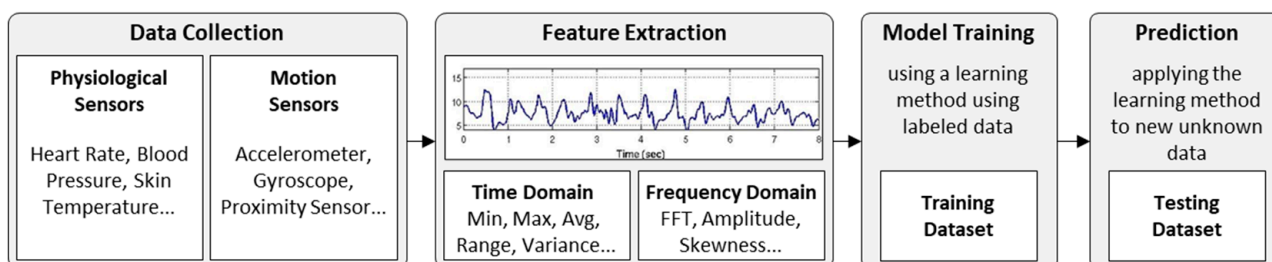


Figure 1. General data-processing flow for HAR.

In the early stages of HAR research, previous studies mainly used two approaches to extract features from time-series data: statistical and structural [31]. These approaches are hand-crafted methods that transform the raw data into particular pre-defined descriptors [32]. Hand-made features and shallow learning algorithms have been used to classify activities [33]. A shallow learning algorithm can be defined by the low depth of the paths of trainable units between the input and output layers [34]. When the low depth of a shallow learning algorithm becomes deeper, the algorithm turns to deep learning architecture. Recently, there have been lots of deep learning approaches for wearable sensor-based HAR [35–39].

In the early stages of applying deep learning methods, deep belief networks (DBNs) were used [40]. DBNs were built by staking multiple layers of a restricted Boltzmann machine (RBM). Afterwards, DBN-based models implemented a hidden Markov model (HMM) on top of the RBM layer to exploit the unique temporal sequences of human activity [41]. However, HMMs are limited by the number of possible hidden states and are impractical when modeling long-range dependencies in large context windows. Zeng et al. [42] proposed convolutional neural networks (CNNs) for HAR. Although the suggested model presented the possibility of the CNN model for HAR [42], they used a shallow model, not a deep learning model. CNN models using a deep learning model can classify various human activities because CNN models can learn robust and identifiable features and capture local dependencies between nearby input samples by utilizing convolution over one-dimensional time sequences [29,43]. CNNs use time-dependent parameter sharing and local connections between adjacent layers to capture local dependencies [44]. However, sharing parameters over time is insufficient to capture all correlations between input samples. Local connectivity limits the output in a function of a small number of neighboring input samples [45–47].

A DRNN model was proposed to utilize the internal memory to capture the temporal dynamics of the activity sequence. Inoue et al. [48] optimized DRNN to achieve high throughput and short recognition time. In particular, the authors proved that the DRNN model is a suitable method for HAR by comparing the time taken by the existing shallow learning models such as support vector machine (SVM) and decision tree with the time taken by the optimized DRNN model. In addition, when using only DRNN without using CNN in HAR, DRNN has the advantage of responding to window sizes of various lengths instead of the fixed-length window size required by CNN. Considering that the length of the gait pattern (i.e., stride length) varies from individual to individual, it is judged that the

DRNN model can distinguish between normal gaits and abnormal gaits. A representative study that showed this possibility is the study of Murad and Pyun [45]. This study proposed a unidirectional, bidirectional, and cascaded long short-term memory (LSTM) architecture based on data collected from wearable sensors. All three methods showed excellent HAR performance, but the author decided to apply the cascaded LSTM-DRNN model in this study. The reason for using this model is that Murad and Pyun [45] showed a higher F1 score compared to KNN or CNN in the Daphnet Freezing of Gait Data Set (Daphnet Fog), which is data for classifying gait patterns in people with Parkinson's disease.

This study aims to identify the environmental barrier through the classification of normal gaits and abnormal gaits caused by the environmental barrier using wearable sensor data. To this end, the author labels and applies the experimental data performed in the author's previous study [27] to the cascaded LSTM-based DRNN model [45,49] for training and testing the model. Afterward, the feasibility of the model for new data is checked by applying the data of the experiments conducted at the same site to the built model.

The remaining parts of this paper are organized as follows: Section 2 introduces the methodology, including how the wearable sensor-based gait data collects, how the cascaded LSTM-based DRNN model is composed, and how the model is trained and tested. Section 3 illustrates the results of (1) testing and training the model and (2) investigating the relationship between the presence of an environmental barrier and HAR results (normal/abnormal gaits). Several discussion points are presented in Section 4. Section 5 wraps up this study and suggests future research.

2. Methodology

2.1. Research Framework

Figure 2 illustrates the research framework. The framework proposed in this study is mainly composed of four parts. The first part is data collection using a wearable device from participants (i.e., a chest-mounted camcorder for collecting ground truth, a pocket held smartphone for tracking the participant's location using a global positioning system (GPS), and an ankle attached IMU sensor for securing 3-degree of acceleration and angular velocity respectively). Second, the experimenter attaches the equipment and walks along the set path at the test site, and the attached equipment collects data in this process. The data collection process in this study can be divided into two main categories. In the author's previous study, 101,607 gaits were collected from 64 participants on the same site. The previously collected data is used to train and test the cascaded LSTM-based DRNN model. In addition, to check whether the cascaded LSTM-based DRNN model constructed in this study is feasible even for new data, 31,142 gaits collected through other subjects in the same experiment were collected. All data collected were obtained from O'Connor et al. After classifying them into individual gaits through the gait detection algorithm proposed by O'Connor et al. [50], they were labeled as normal gaits and abnormal gaits according to the ground truth and gait pattern. The third part determines the number of hidden layers by inputting the gait data collected in the previous study into the cascaded LSTM-based DRNN model. The data collected in the previous study are processed by dividing it into training data (80%) and test data (20%) through random sampling. The last part performs activity classification on the proposed model by using the newly collected data in this study as test data and finally confirms the relationship between the classification results and the environmental barrier. In the following sections, the details of each part will be elaborated on.

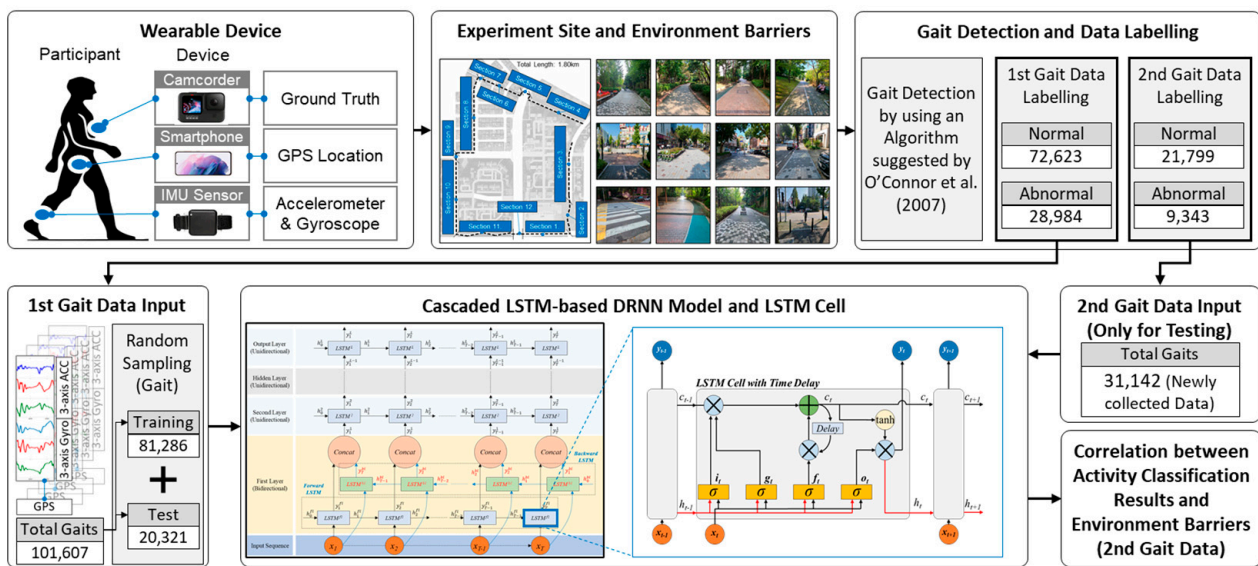


Figure 2. Research Framework.

2.2. Experiment Design and Data Collection

To achieve the purpose of this study, participants were recruited twice, and they were asked to walk a distance of 1.80 km while wearing the three types of equipment presented above. All the subjects participated in this study after giving informed consent approved by the Dankook University Institutional Review Board. In the informed consent, there were detailed explanations including the objectives of the experiment, the experimental procedure, and the right to stop the experiment whenever a subject wants to. The experimental site was the same as the site of the author’s previous study, and Figure 3 presents a graphical summary of the previous study. The experimental site’s data collection process and environmental features are presented in detail in previous studies [27]. In this study, the gait data were collected by a commercial wearable sensor (Opal sensor with 1.15 degree of roll/pitch static accuracy, 1.50 degree of heading static accuracy, 2.80 degree of dynamic accuracy) produced by APDM Inc. In addition, the gait data collected by using this sensor were highly correlated with a motion-tracking system [51].

The first experiment consisted of 64 participants, and the second experiment consisted of a total of 20 participants. Participants in both experiments were different people; those who participated in the first experiment did not participate in the second experiment. To recruit participants from their 20s to 50s, people who were engaged in running club activities were recruited. Members of the senior gateball club were recruited to secure participants aged over 60. A total of 84 people applied, and all volunteers were healthy enough to walk 1.8 km without difficulty.

The participants’ ages and genders in the first and second experiments are presented respectively in Table 1.

Table 1. Age and Gender of Participants.

Age	Participants of 1st Experiment			Participants of 2nd Experiment		
	Male	Female	Total	Male	Female	Total
20s–30s	16	13	29	4	2	6
40s–50s	8	8	16	5	4	9
Over 60s	10	7	17	2	3	5
Total	34	28	64	11	9	20



Figure 3. Graphical summary of experimental site and procedure; (a) site and sections; (b–m) representative pictures of each section; (n) first stage of experiment (data collection); and (o) second stage of experiment (examination and record of environmental barrier expressed by participants).

2.3. Cascaded Unidirectional and Bidirectional LSTM-Based DRNN Model for HAR

A recurrent neural network (RNN) is composed of cyclic connections that can learn the temporal dynamics of sequential data. As the data collected from gaits using an IMU sensor are sequential, RNN may be suitable for classifying normal and abnormal gaits. However, training regular RNNs can be challenging due to vanishing or exploding gradient problems which interfere with the network’s ability to backpropagate gradients over long time intervals [52,53]. To solve this problem, LSTM-based RNNs were suggested [54–56]. However, LSTM-based RNNs can replace traditional nodes with memory cells with internal and outer recurrence to the model temporal sequence and a wide range of dependencies. The architecture of an LSTM cell is presented in Figure 4.

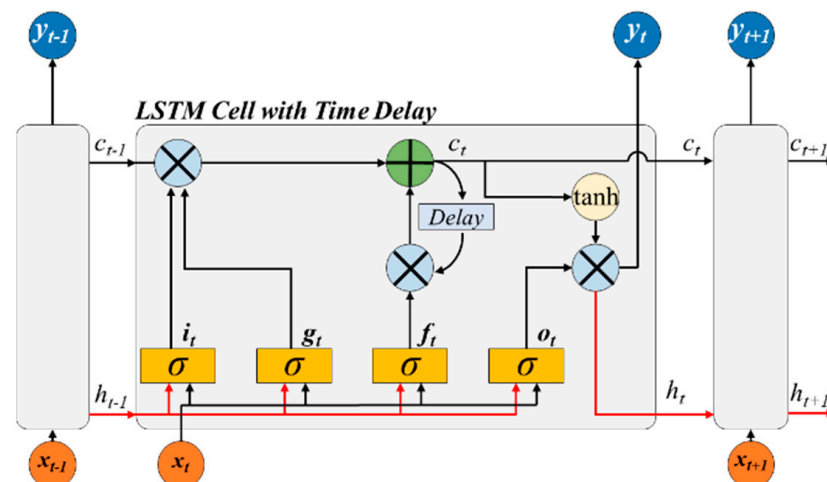


Figure 4. LSTM cell architecture.

The architecture in Figure 4 is defined as the following Equations (1)–(6). The training process of an LSTM-based DRNN is focused on the parameters b , U , and W of the cell gates.

$$f_t = \sigma(W_f x_t + U_f h_{t-1} + b_f) \tag{1}$$

$$i_t = \sigma(W_i x_t + U_i h_{t-1} + b_i) \tag{2}$$

$$o_t = \sigma(W_o x_t + U_o h_{t-1} + b_o) \tag{3}$$

$$g_t = \sigma(W_g x_t + U_g h_{t-1} + b_g) \tag{4}$$

$$c_t = g_t \odot i_t + f_t \odot c_{t-1} \tag{5}$$

$$h_t = \tanh(c_t) \odot o_t \tag{6}$$

The \odot symbol represents the Handarmard product (element-wise multiplication of vectors), and the σ symbol represents the sigmoid function. All the LSTM cells in each layer share the same weights ($W_f, U_f, W_i, U_i, W_o, U_o, W_g, U_g$ and biases b_f, b_i, b_o, b_g). The output of each LSTM cell is used as the input for the next cell. Moreover, the outputs of each LSTM cell in the first layer in the DRNN are fed as inputs to the second layer.

The suggested LSTM-based DRNN model consists of two types of LSTM networks, unidirectional and bidirectional, as shown in Figure 5. The model includes four types of layers in which the first layer is bidirectional and the upper layers (second, hidden, and output layers) are unidirectional RNNs.

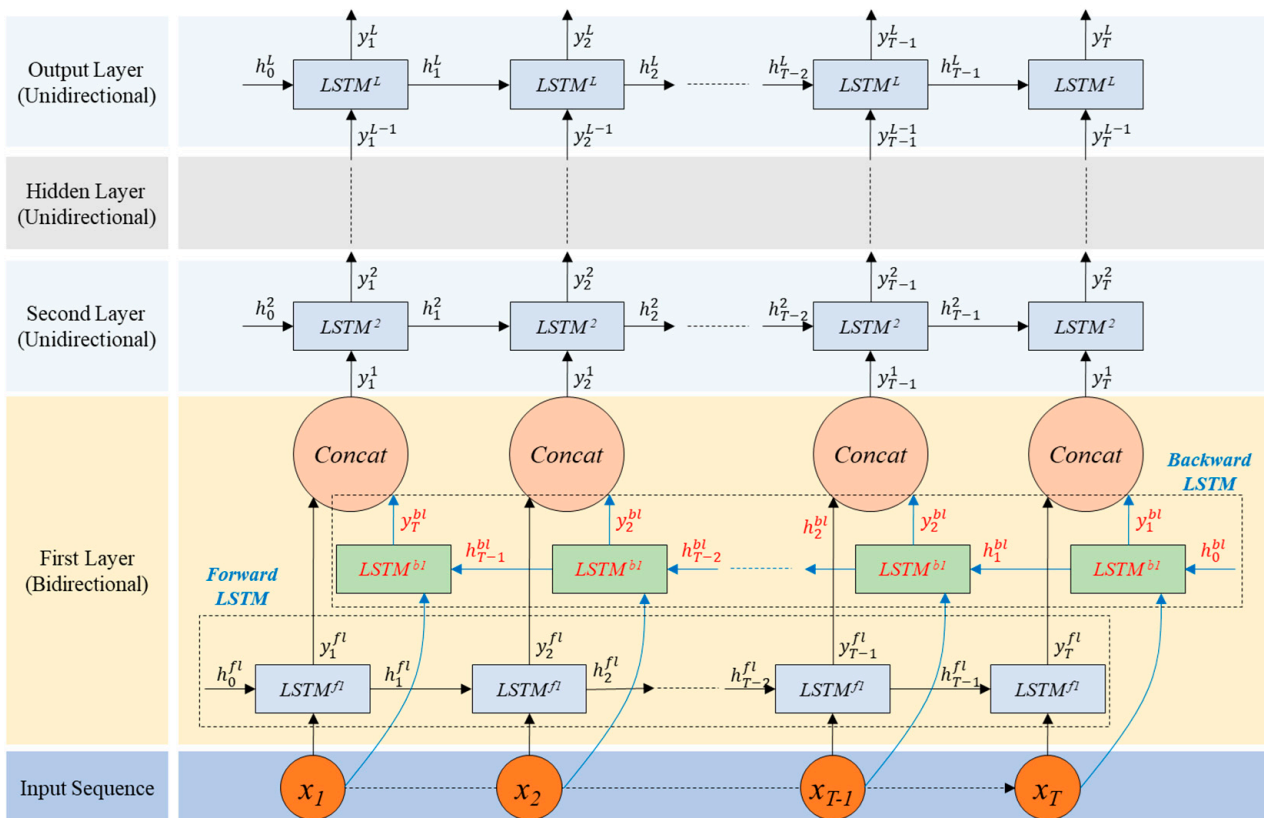


Figure 5. The structure of cascaded unidirectional and bidirectional LSTM-based DRNN.

The first layer includes two parallel LSTM tracks. In the first layer, there are forward LSTMs (sky-blue boxes) and backward LSTMs (green boxes). The sequences such as x_1, x_2, \dots, x_t are inputted in the first layer; the sequences are inputted to forward LSTMs and backward LSTMs, respectively. After inputting sequences, the $LSTM^{fl}$ (forward LSTM) generates an output $(y_1^{fl}, y_2^{fl}, \dots, y_T^{fl})$ and the $LSTM^{bl}$ (backward LSTM) generates an

output $(y_1^{b1}, y_2^{b1}, \dots, y_T^{b1})$. The two types of outputs from forward and backward LSTM are concatenated to generate a new output $(y_1^1, y_2^1, \dots, y_T^1)$ that is inputted into the second layer. This process of bidirectional LSTM follows Equations (7)–(9).

$$y_t^{f1}, h_t^{f1}, c_t^{f1} = LSTM^{f1} (c_{t-1}^{f1}, h_{t-1}^{f1}, x_t; W^{f1}) \quad (7)$$

$$y_t^{b1}, h_t^{b1}, c_t^{b1} = LSTM^{b1} (c_{t-1}^{b1}, h_{t-1}^{b1}, x_t; W^{b1}) \quad (8)$$

$$y_t^1 = y_t^{f1} + y_{T-t+1}^{b1} \quad (9)$$

The second layer is a unidirectional LSTM structure. The concatenated output $(y_1^1, y_2^1, \dots, y_T^1)$ are inputted to the second layer. After inputting the concatenated output, the second, the hidden, and output layers are operated as following a general process of a unidirectional LSTM-based DRNN.

3. Results

3.1. Data Labelling and Model Training/Test using First Dataset

The HAR method for walkability measurement suggested in this study has been validated using the two types of data sets described in the previous section. The suggested LSTM-based DRNN model was trained using 80% of the first data set (64 participants). Then, the rest of the first data set (20% of data) was used to test the training model. While training the model, the binary cross-entropy error between ground truth labels and predicted output labels was used as a cost function because binary cross-entropy error is generally adequate to the backward LSTMs, and the number of label types is two (normal and abnormal gait). The ground truth labels were analyzed by (1) six experts (who were orthopedic surgeons with a specialty in gait analysis) for determining normal and abnormal gaits and (2) the gait detection algorithm [50] for the segmented windows that are fed to the first layer. The labeled data are provided as a one-hot vector.

There are several popular optimization algorithms, such as SGD, RMSProp, AdaGrad, AdaDelta, Adam, Adamax, and Nadam. Nadam was selected to minimize the cost function among these optimization algorithms by backpropagating its gradient and updating model parameters since Nadam outperformed other optimization algorithms in binary classification [57]. To avoid an overfitting problem, both the dropout technique and the batch normalization technique were used [58,59].

Figure 6 presents the accuracy and binary cross-entropy cost of training and testing using the first dataset. As shown in Figure 6a, the gap in accuracy between training and test is very small. In addition, the binary cross entropies of training and test are very similar, as shown in Figure 6b. The results indicate that the Nadam, the dropout technique, and the batch normalization technique effectively generalize the suggested model and avoid an overfitting problem.

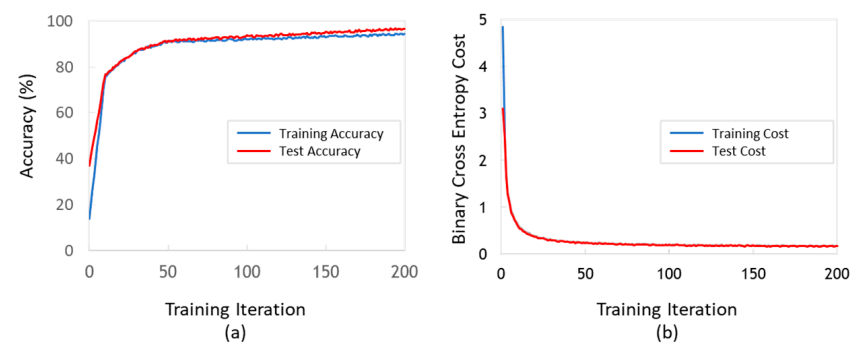


Figure 6. Accuracy and cost of training and testing using the first dataset: (a) accuracies of training (blue line) and test (red line); and (b) binary cross-entropy cost between ground truth and predicted labels for both training (blue line) and test (red line).

3.2. Model Test Using Second Dataset

In the results of training and testing using the first dataset, it may be considered that both accuracy and binary cross-entropy cost are acceptable. However, it is crucial for the suggested model to investigate the feasibility of newly added gait data since the method can be operated for monitoring the conditions of the walking environment where lots of newly added data are generated. In this consideration, the second dataset is inputted into the suggested model. The second dataset was collected at the same experimental site as the first dataset, but not with the same participants. Thus, the second dataset can be used to check whether the trained model is feasible for newly added data. Figure 7 presents the test results using the second dataset. In Figure 7, both test results using the first and second datasets are presented for comparison to each other. The result of the test accuracy of the second dataset is very similar to that of the first dataset, as shown in Figure 7a. Figure 7b presents that there is a small gap between the binary cross-entropy cost of the first dataset (for a test) and that of the second dataset. This comparison between two datasets indicates that the suggested model can be effectively operated using newly added data.

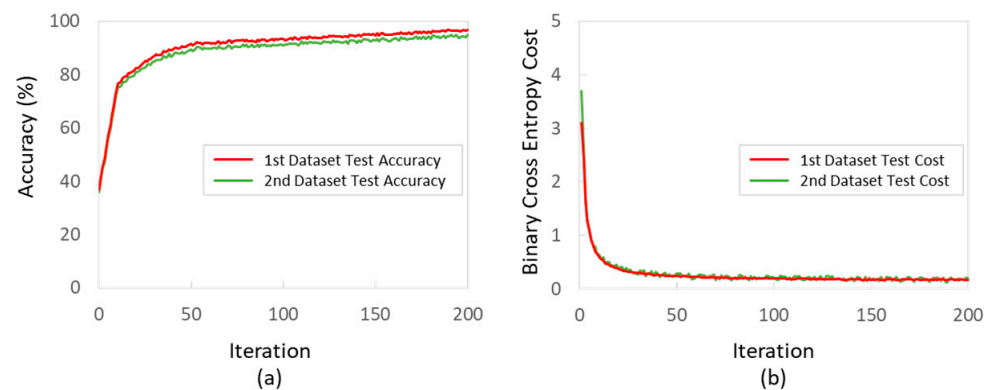


Figure 7. Accuracy and cost of testing using the first and second dataset: (a) accuracy (red line for the first data set and green line for the second dataset); and (b) binary cross-entropy cost between ground truth and predicted labels for test (red line for the first data set and green line for the second dataset).

In this study, two gait classes are used: *Normal Gait* and *Abnormal Gait*. To analyze the performance of the model in more detail, the gait classification results are analyzed. Figure 6 shows the classified activities and performance metrics of both the first and second datasets. The test results of the first dataset as shown in Figure 8a present 96.8% accuracy, 99.2% precision, 96.4% recall, and 0.978 F1-score. The test results of the second dataset also show very similar results to that of the first dataset (see Figure 8b). These two test results with high values of performance metrics such as accuracy, precision, recall, and F-1 score indicate that the suggested model can distinguish between normal and abnormal gaits. This result may lead us to allow the gait classification method to monitor the walking environment and identify environment barriers hindering pedestrians' walkability.

3.3. Investigating of Relationship between Environment Barriers and Gait Classification Results

By analyzing the gait classification results conducted in the previous section, it can be considered that the performance of gait classification is confirmed. However, one more thing is needed to use the proposed pedestrian environment monitoring and environmental barrier identification method. This study investigates the relationship between the presence of environmental barriers and the ratio of abnormal gaits in a specific location.

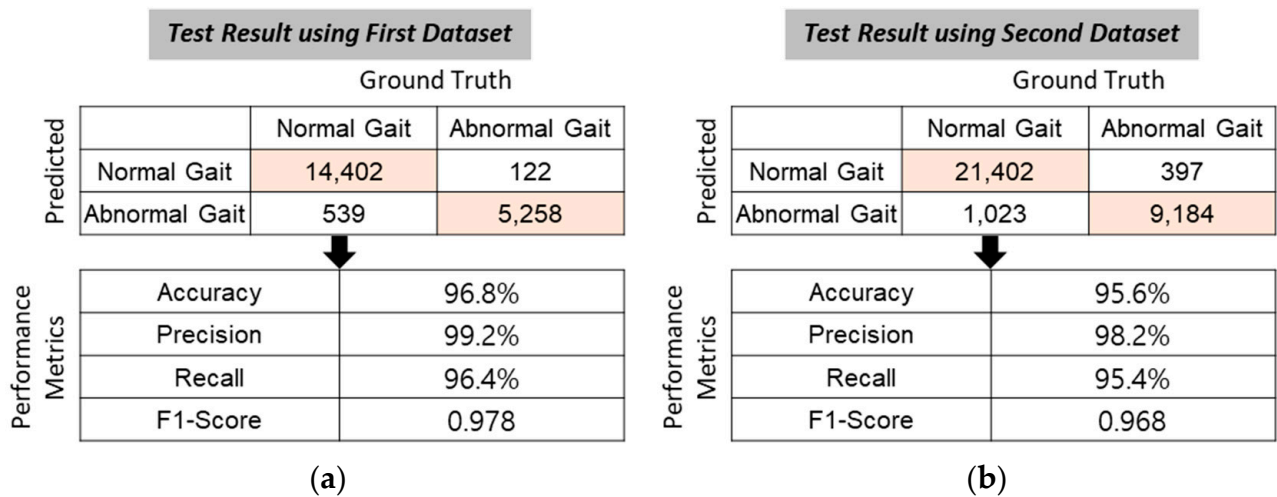


Figure 8. The test results and performance metrics: (a) gait classification results and performance metrics of the test results of the first dataset; and (b) gait classification results and performance metrics of the test results of the second dataset.

To confirm the feasibility of the suggested method, the three relationships between the presence of environment barriers and the ratio of abnormal gaits (ground truth, first dataset, and second dataset, respectively) are measured. The ratio of abnormal gaits in a specific location (cell) is a continuous variable, whereas the presence of environment barriers can be represented as a binary variable (existence as one and absence as zero). To investigate the relationship between the presence of environmental barriers and the ratio of abnormal gaits statistically, the point biserial correlation coefficient is used in this study. This coefficient is usually used when one is dichotomous and the other is continuous [60,61]. The point biserial coefficient is calculated using Equation (10) as follows:

$$r_{pb} = \frac{(M_1 - M_0) \sqrt{(n_1 n_0 / n^2)}}{\sqrt{\frac{1}{n} \sum_{i=1}^n (X_i - \bar{X})^2}} \tag{10}$$

where r_{pb} is the point biserial correlation coefficient, M_1 is the mean value of the continuous variable X (ratio of abnormal gaits) for all data points in group 1 (existence of environment barrier), M_0 is the mean value of the continuous variable X (ratio of abnormal gaits) for all data points in group 2 (absence of environment barrier), n_1 is the number of data points in group 1, n_0 is the number of data points in group 2, and n is the total sample size.

The point biserial coefficient calculation results are presented in Table 2. The three correlation results present correlation coefficients over 0.7 and statistical significance ($\alpha < 0.005$, $p = 0.001$). A correlation coefficient greater than 0.7 indicates a high degree of correlation. The results showed that the ratio of abnormal gaits and the existence (presence and absence) of environmental barriers are highly correlated. These correlation coefficients of the three types of data sources and the existence of environmental barriers are very similar. This means that the suggested method can both (1) classify normal and abnormal gaits and (2) be feasible to newly added data for robust DRNN-based walking environment monitoring.

Table 2. Correlation between environment barriers and three types of ratio of abnormal gaits.

Correlation Coefficient	Ratio of Abnormal Gaits		
	Ground Truth	First Dataset	Second Dataset
Environment Barrier	0.760	0.742	0.735

4. Discussion

4.1. Contributions and Future Applications of the Suggested Method for Walking Environment

Considering the human gait's characteristics, the more abnormal gaits in a specific location may indicate the existence of an environmental barrier to walkability. The suggested method can classify pedestrians' normal and abnormal gaits. If pedestrians' gait data on a daily walking environment are collected, then a certain location with a higher ratio of abnormal gaits than other locations can be a candidate that needs to be investigated. This process can help government agencies to determine how an environmental barrier should be handled. In addition, the suggested method can provide the basis for continuous monitoring of the built environment. Therefore, the major contributions of this study can be summarized as follows:

1. The wearable data show that normal gaits and abnormal gaits in a walking environment can be distinguished through the cascaded LSTM-based DRNN model.
2. In terms of monitoring the walking environment, it is suggested that the built model can distinguish between normal gaits and abnormal gaits even when new data is inputted.
3. In a specific location, the high correlation between the distribution of normal gaits and abnormal gaits and the presence of an environmental barrier is presented.

Various studies have been conducted to measure HAR with the development of various wearable devices including smartphones and smartwatches. In previous studies, the accuracy of analyzing behavior using the accelerometer and gyroscope of smartphones and smart watches is over 90% [62]. This level of accuracy can be applied to walking, and it can be said that it shows the possibility that the method proposed at the application level can be applied in the future.

However, the suggested method should handle a problem related to carrying a sensor. In this study, the data are collected from an IMU sensor attached to a pedestrian's ankle. An IMU sensor attached to an ankle should be replaced with a smartphone to convert the suggested method to a real-world application. In a smartphone, there are various sensors, including a 9-degree of IMU and a function to transfer collected data to a server. If pedestrians' data collection through a smartphone is possible, conditions of the walking environment can be collected and analyzed in real-time. Although the strengths of using a smartphone for monitoring the walking environment are evident, privacy issues should be handled in future studies.

4.2. Effects of the Environment Barriers' Characteristics

This study proposes a method for classifying pedestrians' gaits (normal and abnormal) and identifying environmental barriers based on a cascaded unidirectional and bidirectional LSTM-based DRNN. For this purpose, data generated from walking was used. In the analysis, there are normal gaits even on an environmental barrier. Depending on the size and location of the environmental barrier, it may affect walkability or gait pattern. Figure 7 is an example showing how the response can change depending on the size and location of the environment barrier. In this study, the authors compare the effects by paying attention to the characteristics (location, width, and depth) of three types of environmental barriers.

Figure 9a compares environmental barriers with different widths. When the depth of the two environmental barriers is less than the step length, the representative action that pedestrians can take is crossing or avoiding the environmental barrier. When crossing the environmental barrier, it appears similarly regardless of the width in both cases in Figure 9a. However, when avoiding the environmental barrier, when the environmental barrier is wide, abnormal gaits may appear higher than when the width of the environment barrier is good due to insufficient width of the pathway.

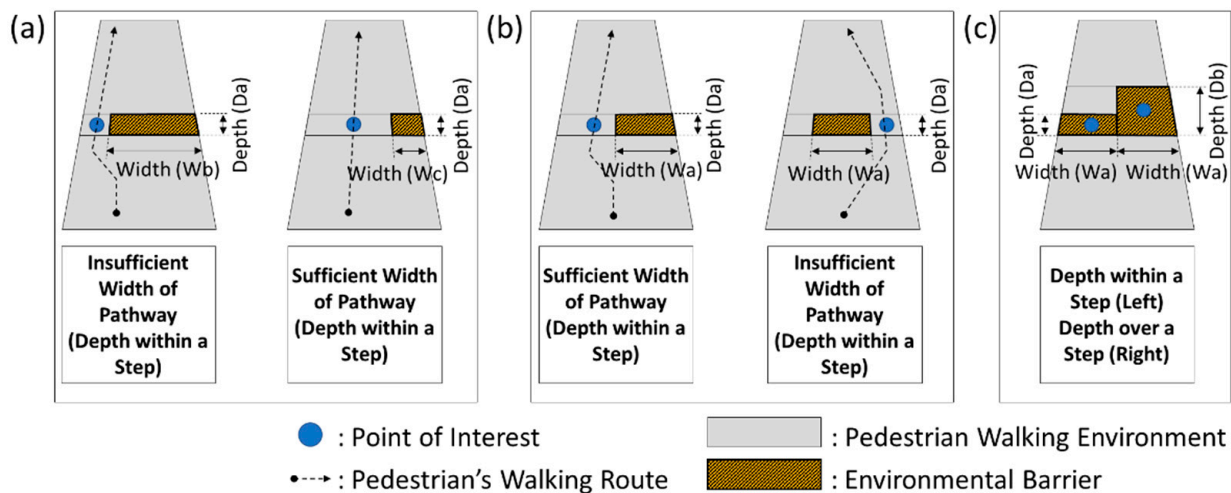


Figure 9. Comparison of Effects by Size and Location of Environmental Barriers: (a) Comparison of Location of Environmental Barrier; (b) Comparison of Width of Environmental Barrier; and (c) Comparison of Depth of Environmental Barrier.

Figure 9b compares the location of an environmental barrier of the same size. Even an environmental barrier of the same size can affect the gait depending on the location. A sufficient walking path can be secured if the environment barrier is located on one side (Figure 9b left). As a result, the rate of abnormal gait can be measured relatively low. On the other hand, a relatively high rate of abnormal gaits may appear when the environment barrier is located in the middle of the pedestrian path and insufficient width of the gait on both sides is secured (Figure 9b right).

Figure 9c compares environmental barriers with different depths. If the depth of the environmental barrier is less than the stride length, a pedestrian can easily jump over it, but otherwise (if the depth exceeds the stride length), you have to jump over it. This difference in behavior results in the different ratio of abnormal gaits in a specific location.

Even similar environmental barriers can cause different reactions depending on their size and location. Therefore, there is a need to perform built environment monitoring based on the reaction between environmental barriers and pedestrians, beyond finding the presence or absence of environmental barriers.

5. Conclusions

Monitoring the walking environment is essential for pedestrians. Conventional approaches to identify environment barriers have several limitations: time-consuming, labor-intensive, and discontinuous inspection. This study suggests a cascaded unidirectional and bidirectional LSTM-based DRNN model using pedestrians' gait data collected from a wearable sensor to overcome these limitations. To determine a model and investigate the feasibility for a real-world application, this study uses two gait datasets sourced from two data collections. A total of 132,749 gaits were used in this study. The suggested model was trained using 81,286 gaits and tested twice using the first dataset (20,321 gaits) and the second dataset (31,142 gaits). The results of the model tests showed high accuracy, precision, recall, and F1 score. Even more, abnormal gaits (ground truth labels, the first dataset, and the second dataset) and the presence of environmental barriers are highly correlated. The high correlation coefficients indicate the potential of the suggested method to identify environmental barriers. In summary, the suggested method shows the ability to classify normal and abnormal gaits of 84 participants and the feasibility to derive reasonable outputs for newly added data.

Funding: The present research was supported by the research fund of Dankook university in 2019 (grant number: R201901448).

Institutional Review Board Statement: The study was conducted according to the guidelines of the Declaration of Helsinki, and approved by the Institutional Review Board of DANKOOK UNIVERSITY (DKU 2020-09-027, date of approval 14 September 2020).

Informed Consent Statement: Informed consent was obtained from all subjects involved in the study.

Data Availability Statement: Some or all data, or code generated during the study, are proprietary or confidential in nature and may only be provided with restrictions (e.g., anonymized data).

Acknowledgments: The author wishes to acknowledge Sunghyun Yoon, director of Jungja Running Club, Jung-Ae Oh, director of Jungja 2 Dong Gateball Club, and all the participants for their help in data collection.

Conflicts of Interest: The author declares no conflict of interest. The funders had no role in the design of the study; in the collection, analyses, or interpretation of data; in the writing of the manuscript, or in the decision to publish the results.

References

- Bell, S.L.; Audrey, S.; Gunnell, D.; Cooper, A.; Campbell, R. The relationship between physical activity, mental wellbeing and symptoms of mental health disorder in adolescents: A cohort study. *Int. J. Behav. Nutr. Phys. Act.* **2019**, *16*, 138. [[CrossRef](#)]
- Nielsen, J.B. How we walk: Central control of muscle activity during human walking. *Neuroscientist* **2003**, *9*, 195–204. [[CrossRef](#)] [[PubMed](#)]
- Nilsson, J.; Thorstensson, A.; Halbertsma, J.N. Changes in leg movements and muscle activity with speed of locomotion and mode of progression in humans. *Acta Physiol. Scand.* **1985**, *123*, 457–475. [[CrossRef](#)] [[PubMed](#)]
- Frank, L.D.; Kerr, J.; Sallis, J.F.; Miles, R.; Chapman, J. A hierarchy of sociodemographic and environmental correlates of walking and obesity. *Prev. Med.* **2008**, *47*, 172–178. [[CrossRef](#)] [[PubMed](#)]
- Browning, R.C.; Baker, E.A.; Herron, J.A.; Kram, R. Effects of obesity and sex on the energetic cost and preferred speed of walking. *J. Appl. Physiol.* **2006**, *100*, 390–398. [[CrossRef](#)] [[PubMed](#)]
- Levine, J.A.; McCrady, S.K.; Lanningham-Foster, L.M.; Kane, P.H.; Foster, R.C.; Manohar, C.U. The role of free-living daily walking in human weight gain and obesity. *Diabetes* **2008**, *57*, 548–554. [[CrossRef](#)] [[PubMed](#)]
- Smith, T.C.; Wingard, D.L.; Smith, B.; Kritiz-Silverstein, D.; Barrett-Connor, E. Walking decreased risk of cardiovascular disease mortality in older adults with diabetes. *J. Clin. Epidemiol.* **2007**, *60*, 309–317. [[CrossRef](#)] [[PubMed](#)]
- Hu, F.B.; Sigal, R.J.; Rich-Edwards, J.W.; Colditz, G.A.; Solomon, C.G.; Willett, W.C.; Speizer, F.E.; Manson, J.E. Walking compared with vigorous physical activity and risk of type 2 diabetes in women: A prospective study. *Jama* **1999**, *282*, 1433–1439. [[CrossRef](#)]
- Murtagh, E.M.; Murphy, M.H.; Boone-Heinonen, J. Walking—the first steps in cardiovascular disease prevention. *Curr. Opin. Cardiol.* **2010**, *25*, 490. [[CrossRef](#)]
- Johnson, S.T.; Bell, G.J.; McCargar, L.J.; Welsh, R.S.; Bell, R.C. Improved cardiovascular health following a progressive walking and dietary intervention for type 2 diabetes. *Diabetes Obes. Metab.* **2009**, *11*, 836–843. [[CrossRef](#)]
- Fisher, K.J.; Li, F. A community-based walking trial to improve neighborhood quality of life in older adults: A multilevel analysis. *Ann. Behav. Med.* **2004**, *28*, 186–194. [[CrossRef](#)] [[PubMed](#)]
- Blacklock, R.E.; Rhodes, R.E.; Brown, S.G. Relationship between regular walking, physical activity, and health-related quality of life. *J. Phys. Act. Health* **2007**, *4*, 138–152. [[CrossRef](#)] [[PubMed](#)]
- Rosenberg, D.E.; Huang, D.L.; Simonovich, S.D.; Belza, B. Outdoor built environment barriers and facilitators to activity among midlife and older adults with mobility disabilities. *Gerontologist* **2013**, *53*, 268–279. [[CrossRef](#)] [[PubMed](#)]
- Lee, G.; Choi, B.; Jebelli, H.; Ahn, C.R.; Lee, S. Wearable biosensor and collective sensing-based approach for detecting older adults' environmental barriers. *J. Comput. Civ. Eng.* **2020**, *34*, 04020002. [[CrossRef](#)]
- Kim, H.; Ahn, C.R.; Yang, K. A people-centric sensing approach to detecting sidewalk defects. *Adv. Eng. Inform.* **2016**, *30*, 660–671. [[CrossRef](#)]
- Kim, J.; Ahn, C.R.; Nam, Y. The influence of built environment features on crowdsourced physiological responses of pedestrians in neighborhoods. *Comput. Environ. Urban Syst.* **2019**, *75*, 161–169. [[CrossRef](#)]
- Resch, B.; Puetz, I.; Bluemke, M.; Kyriakou, K.; Miksch, J. An interdisciplinary mixed-methods approach to analyzing urban spaces: The case of urban walkability and bikeability. *Int. J. Environ. Res. Public Health* **2020**, *17*, 6994. [[CrossRef](#)]
- Arya, D.; Maeda, H.; Ghosh, S.K.; Toshniwal, D.; Mraz, A.; Kashiya, T.; Sekimoto, Y. Deep learning-based road damage detection and classification for multiple countries. *Autom. Constr.* **2021**, *132*, 103935. [[CrossRef](#)]
- Ham, Y.; Han, K.K.; Lin, J.J.; Golparvar-Fard, M. Visual monitoring of civil infrastructure systems via camera-equipped Unmanned Aerial Vehicles (UAVs): A review of related works. *Vis. Eng.* **2016**, *4*, 1. [[CrossRef](#)]
- Koch, C.; Brilakis, I. Pothole detection in asphalt pavement images. *Adv. Eng. Inform.* **2011**, *25*, 507–515. [[CrossRef](#)]
- Rantakokko, M.; Törmäkangas, T.; Rantanen, T.; Haak, M.; Iwarsson, S. Environmental barriers, person-environment fit and mortality among community-dwelling very old people. *BMC Public Health* **2013**, *13*, 783. [[CrossRef](#)] [[PubMed](#)]
- Iwarsson, S.; Nygren, C.; Oswald, F.; Wahl, H.-W.; Tomsone, S. Environmental barriers and housing accessibility problems over a one-year period in later life in three European countries. *J. Hous. Elder.* **2006**, *20*, 23–43. [[CrossRef](#)]

23. Lee, G.; Choi, B.; Ahn, C.R.; Lee, S. Wearable biosensor and hotspot analysis-based framework to detect stress hotspots for advancing elderly's mobility. *J. Manag. Eng.* **2020**, *36*, 04020010. [[CrossRef](#)]
24. Bisadi, M.; Kim, H.; Ahn, C.R.; Nam, Y. Effects of physical disorders in neighborhoods on pedestrians' physiological responses. In *Computing in Civil Engineering 2017*; ASCE: Seattle, WA, USA, 2017; pp. 183–190.
25. Kim, J.; Yadav, M.; Chaspari, T.; Ahn, C.R. Saliency detection analysis of collective physiological responses of pedestrians to evaluate neighborhood built environments. *Adv. Eng. Inform.* **2020**, *43*, 101035. [[CrossRef](#)]
26. Zeile, P. Defining and assessing walkability: A concept for an integrated approach using surveys, biosensors and geospatial analysis. *Urban Dev. Issues* **2019**, *62*, 5–15.
27. Lee, B.; Kim, H. Two-Step k-means Clustering Based Information Entropy for Detecting Environmental Barriers Using Wearable Sensor. *Int. J. Environ. Res. Public Health* **2022**, *19*, 704. [[CrossRef](#)]
28. Lee, B.; Hwang, S.; Kim, H. The Feasibility of Information-Entropy-Based Behavioral Analysis for Detecting Environmental Barriers. *Int. J. Environ. Res. Public Health* **2021**, *18*, 11727. [[CrossRef](#)]
29. Lara, O.D.; Labrador, M.A. A survey on human activity recognition using wearable sensors. *IEEE Commun. Surv. Tutor.* **2012**, *15*, 1192–1209. [[CrossRef](#)]
30. Bulling, A.; Blanke, U.; Schiele, B. A tutorial on human activity recognition using body-worn inertial sensors. *ACM Comput. Surv.* **2014**, *46*, 1–33. [[CrossRef](#)]
31. Ignatov, A. Real-time human activity recognition from accelerometer data using Convolutional Neural Networks. *Appl. Soft Comput.* **2018**, *62*, 915–922. [[CrossRef](#)]
32. Munoz-Organero, M. Outlier detection in wearable sensor data for human activity recognition (HAR) based on DRNNs. *IEEE Access* **2019**, *7*, 74422–74436. [[CrossRef](#)]
33. Sargano, A.B.; Angelov, P.; Habib, Z. A comprehensive review on handcrafted and learning-based action representation approaches for human activity recognition. *Appl. Sci.* **2017**, *7*, 110. [[CrossRef](#)]
34. Schmidhuber, J. Deep learning in neural networks: An overview. *Neural Netw.* **2015**, *61*, 85–117. [[CrossRef](#)] [[PubMed](#)]
35. Bianchi, V.; Bassoli, M.; Lombardo, G.; Fornacciarri, P.; Mordonini, M.; De Munari, I. IoT wearable sensor and deep learning: An integrated approach for personalized human activity recognition in a smart home environment. *IEEE Internet Things J.* **2019**, *6*, 8553–8562. [[CrossRef](#)]
36. Ravi, D.; Wong, C.; Lo, B.; Yang, G.-Z. A deep learning approach to on-node sensor data analytics for mobile or wearable devices. *IEEE J. Biomed. Health Inform.* **2016**, *21*, 56–64. [[CrossRef](#)] [[PubMed](#)]
37. Zhang, S.; Li, Y.; Zhang, S.; Shahabi, F.; Xia, S.; Deng, Y.; Alshurafa, N. Deep Learning in Human Activity Recognition with Wearable Sensors: A Review on Advances. *Sensors* **2022**, *22*, 1476. [[CrossRef](#)] [[PubMed](#)]
38. Ramanujam, E.; Perumal, T.; Padmavathi, S. Human activity recognition with smartphone and wearable sensors using deep learning techniques: A review. *IEEE Sens. J.* **2021**, *21*, 13029–13040. [[CrossRef](#)]
39. Janarthanan, R.; Doss, S.; Baskar, S. Optimized unsupervised deep learning assisted reconstructed coder in the on-nodule wearable sensor for human activity recognition. *Measurement* **2020**, *164*, 108050. [[CrossRef](#)]
40. Ji, S.; Xu, W.; Yang, M.; Yu, K. 3D convolutional neural networks for human action recognition. *IEEE Trans. Pattern Anal. Mach. Intell.* **2012**, *35*, 221–231. [[CrossRef](#)]
41. Alsheikh, M.A.; Selim, A.; Niyato, D.; Doyle, L.; Lin, S.; Tan, H.-P. Deep activity recognition models with triaxial accelerometers. In Proceedings of the Workshops at the Thirtieth AAAI Conference on Artificial Intelligence, Phoenix, AZ, USA, 12–17 February 2016.
42. Zeng, M.; Nguyen, L.T.; Yu, B.; Mengshoel, O.J.; Zhu, J.; Wu, P.; Zhang, J. Convolutional neural networks for human activity recognition using mobile sensors. In Proceedings of the 6th International Conference on Mobile Computing, Applications and Services, Austin, TX, USA, 6–7 November 2014; IEEE: Manhattan, NY, USA, 2014; pp. 197–205.
43. Jordao, A.; Nazare Jr, A.C.; Sena, J.; Schwartz, W.R. Human activity recognition based on wearable sensor data: A standardization of the state-of-the-art. *arXiv* **2018**, arXiv:1806.05226.
44. Shen, T.; Zhou, T.; Long, G.; Jiang, J.; Pan, S.; Zhang, C. Disan: Directional self-attention network for rnn/cnn-free language understanding. In Proceedings of the AAAI Conference on Artificial Intelligence, New Orleans, LA, USA, 2–7 February 2018; Volume 32.
45. Murad, A.; Pyun, J.-Y. Deep recurrent neural networks for human activity recognition. *Sensors* **2017**, *17*, 2556. [[CrossRef](#)] [[PubMed](#)]
46. Jaouedi, N.; Boujnah, N.; Bouhlel, M.S. A new hybrid deep learning model for human action recognition. *J. King Saud Univ.-Comput. Inf. Sci.* **2020**, *32*, 447–453. [[CrossRef](#)]
47. Liciotti, D.; Bernardini, M.; Romeo, L.; Frontoni, E. A sequential deep learning application for recognising human activities in smart homes. *Neurocomputing* **2020**, *396*, 501–513. [[CrossRef](#)]
48. Inoue, M.; Inoue, S.; Nishida, T. Deep recurrent neural network for mobile human activity recognition with high throughput. *Artif. Life Robot.* **2018**, *23*, 173–185. [[CrossRef](#)]
49. Wu, Y.; Schuster, M.; Chen, Z.; Le, Q.V.; Norouzi, M.; Macherey, W.; Krikun, M.; Cao, Y.; Gao, Q.; Macherey, K. Google's neural machine translation system: Bridging the gap between human and machine translation. *arXiv* **2016**, arXiv:1609.08144.
50. O'Connor, C.M.; Thorpe, S.K.; O'Malley, M.J.; Vaughan, C.L. Automatic detection of gait events using kinematic data. *Gait Posture* **2007**, *25*, 469–474. [[CrossRef](#)] [[PubMed](#)]

51. Yang, K.; Ahn, C.R.; Kim, H. Validating ambulatory gait assessment technique for hazard sensing in construction environments. *Autom. Constr.* **2019**, *98*, 302–309. [[CrossRef](#)]
52. Vorontsov, E.; Trabelsi, C.; Kadoury, S.; Pal, C. On orthogonality and learning recurrent networks with long term dependencies. In Proceedings of the International Conference on Machine Learning, PMLR, Sydney, Australia, 6–11 August 2017; pp. 3570–3578.
53. Balduzzi, D.; Frean, M.; Leary, L.; Lewis, J.P.; Ma, K.W.-D.; McWilliams, B. The shattered gradients problem: If resnets are the answer, then what is the question? In Proceedings of the International Conference on Machine Learning, PMLR, Sydney, Australia, 6–11 August 2017; pp. 342–350.
54. Chen, Y.; Liu, S.; He, S.; Liu, K.; Zhao, J. Event extraction via bidirectional long short-term memory tensor neural networks. In *Chinese Computational Linguistics and Natural Language Processing Based on Naturally Annotated Big Data*; Springer: Berlin/Heidelberg, Germany, 2016; pp. 190–203.
55. Manawadu, U.E.; Kawano, T.; Murata, S.; Kamezaki, M.; Muramatsu, J.; Sugano, S. Multiclass classification of driver perceived workload using long short-term memory based recurrent neural network. In Proceedings of the 2018 IEEE Intelligent Vehicles Symposium (IV), Suzhou, China, 26–30 June 2018; IEEE: Manhattan, NY, USA, 2018; pp. 1–6.
56. Salloum, R.; Kuo, C.-C.J. ECG-based biometrics using recurrent neural networks. In Proceedings of the 2017 IEEE International Conference on Acoustics, Speech and Signal Processing (ICASSP), New Orleans, LA, USA, 5–9 March 2017; IEEE: Manhattan, NY, USA, 2017; pp. 2062–2066.
57. Dogo, E.M.; Afolabi, O.J.; Nwulu, N.I.; Twala, B.; Aigbavboa, C.O. A comparative analysis of gradient descent-based optimization algorithms on convolutional neural networks. In Proceedings of the 2018 International Conference on Computational Techniques, Electronics and Mechanical Systems (CTEMS), Belgaum, India, 21–22 December 2018; IEEE: Manhattan, NY, USA, 2018; pp. 92–99.
58. Cooijmans, T.; Ballas, N.; Laurent, C.; Gülçehre, Ç.; Courville, A. Recurrent batch normalization. *arXiv* **2016**, arXiv:1603.09025.
59. Pham, V.; Bluche, T.; Kermorvant, C.; Louradour, J. Dropout improves recurrent neural networks for handwriting recognition. In Proceedings of the 2014 14th International Conference on Frontiers in Handwriting Recognition, Crete, Greece, 1–4 September 2014; IEEE: Crete, Greece, 2014; pp. 285–290.
60. Holley, J.W.; Berhagen, K.-E. *A Note on the Use of the Point Biserial Correlation Coefficient*; Lund University: Lund, Sweden, 1969.
61. Bobko, P. *Correlation and Regression: Applications for Industrial Organizational Psychology and Management*; Thousand Oak California; Sage Publications: Thousand Oaks, CA, USA, 2001.
62. Demrozi, F.; Pravadelli, G.; Bihorac, A.; Rashidi, P. Human activity recognition using inertial, physiological and environmental sensors: A comprehensive survey. *IEEE Access* **2020**, *8*, 210816–210836. [[CrossRef](#)]